Applied Mechanics and Materials *Online: 2012-01-24*
ISSN: 1662-7482, Vols. 152-154, pp 1244-1249
doi:10.4028/www.scientific.net/AMM.152-154.1244

Epitaxial Growth of Ni-based Superalloys Using Laser and Spark Deposition

Santos, E.C.[1,a], K. Kida[1,2,b], Rozwadowska, J.[1,c], [3,d]Kidera, M., [4,e]Chen, C.

[1] Kyushu University, 744 Motooka, Nishi-ku, Fukuoka 819-0395, Japan

[2] Fundamental Studies on Technologies for Steel Materials with Enhanced Strength and Functions, Consortium of the JRCM, Minato-ku, Tokyo, Japan

[3] Aichi Sangyo co. Ltd., 2-6-8 Higashiooi Shinagawaku, Japan

[4] School of Mechanical and Electrical Engineering, Soochow University , Suzhou, China

[a]santos@mech.kyushu-u.ac.jp, [b]kida@mech.kyushu-u.ac.jp, ,
[c]j.rozwadowska@mech.kyushu-u.ac.jp, [d]kidera@aichi-sangyo.co.jp, [e]chjchen200[illegible]@yahoo.com.cn

Keywords: Ni-based single crystal, epitaxial growth, spark deposition, laser deposition

Abstract. In this paper, epitaxial growth on Ni-based single crystals was achieved by using spark deposition and laser powder deposition. Different Ni-based substrates such as CMSX-4, TMS 138A as well as deposition materials: NiCrAl, Rene N4 and modified 4.5th generation single crystal alloys were used. The deposited layers were analysed by laser confocal microscopy, FEG-SEM, X-ray and electron backscatter diffraction (EBSD), had very little dilution and epitaxial growth was confirmed for the deposits made using Rene N4 electrodes. The deposition time at 100 V voltage, 850 W power and 110 Hz frequency was 3min and the layer thickness varied from 0.3 to 0.5 mm. Cracks were observed in certain areas with the formation of new grains. In order to investigate the influence of the laser processing during multiple build up, specimens with one and ten layers were manufactured. The total layer thickness on substrates was 0.3 mm and 2 mm, respectively. The processing parameters were: laser power of 500 W, laser beam diameter of 0.6 mm and the z displacement was equal to 80% of the layer height. The laser deposition also resulted in successful epitaxial growth and minimal defects (pores or cracks), however the clad presented high dilution.

Introduction

Excellent performance at high temperatures is of fundamental importance for highly efficient energy conversion and longer component service life of gas turbines. The principal requirements are adequate mechanical properties and microstructural stability at high temperature, and good oxidation/corrosion resistance [1]. The use of single-crystalline materials allowed increasing the environmental temperature of critical components such as turbine blades and vanes in the hot section of gas turbines, leading to a major advance in their energetic efficiency [1-3]. Today single crystalline components are successfully produced from Ni-based superalloys by investment casting [1-5], but this technique cannot be used for refractory alloys and intermetallics, due to their high melting temperature and poor castability.

The microstructure of the single crystal Ni-based superalloys is composed of an ordered FCC A_3B (γ' phase) intermetallic phase (A = Ni, B = Al, Ti) dispersed in a disordered matrix that consists of FCC Ni-based solid solution strengthened by substitutional Co, Cr, Mo, W, Ta and Re alloying elements (γ phase) [2,3]. The high temperature strength of the superalloys is controlled mainly by volume fraction, size, spacing and morphology of the intermetallic phase. The earliest precipitation strengthened material (e.g. Nimonic 80 and 90) contained about 10% by volume of the γ′ phase compared to 60 ~ 70 vol% in the modern single crystal superalloys (e.g. CMSX-4 and Rene 4) [4]. Aluminium and chromium are the most important elements that improve oxidation resistance by forming stable oxide scales e.g. Al_2O_3 and Cr_2O_3. On the other hand, chromium tends to lower the γ' solvus temperature and is also responsible for the formation of undesirable embrittling topologically close-packed (TCP)

RETRACTED

phases, such as σ, μ. In order to avoid these drawbacks, the amount of chromium was decreased in the second and third generation single crystal alloys. High temperature strength (high vol% of cuboid shaped γ' phase) and good corrosion resistance (high vol% of Aluminium and Chromium) are conflicting requirements, difficult to optimise. Application of corrosion resistant coatings can overcome this conflict. The coatings should be single crystal to eliminate the diffusion short circuit through grain boundaries.

The high cost of single crystal turbine blades, vanes and seal segments is a major problem and developing a repair method capable of extending their lifetime is a matter of great economic interest. Conventional welding methods such as gas-tungsten-arc welding lead to stray grain formation and cracking [4], alternative repair methods are therefore required.

The coats produced by high-energy micro-arc alloying (HEMAA) are typically free of pores and cracks and their oxidation resistance is usually better compared to coatings produced by other methods [5]. HEMAA gives the possibility to generate coats with high density and almost zero porosity. In addition, it can be used to treat comparable small components and/or components with complex geometry. Moreover, production of functional layers for new parts as well as reconditioning processes of used parts is possible. Hence, HEMAA can be a competitive process to other coating techniques [6].

In Laser Powder Deposition (also referred to as Direct Metal Deposition or Laser Cladding), an object is formed layer by layer by injecting powder into the laser-generated melt pool while scanning the laser beam under CN control, according to a CAD model. The process allows rapid and accurate addition of controlled amounts of material at desired locations with minimum heat input, thus enabling crack-sensitive materials such as Ni-base alloys to be deposited. By controlling the laser power density, laser scan speed and processing parameters, it is possible to deposit single crystal layers free of defects (cracks or pores). As a result, laser powder deposition presents considerable potential as a method for high temperature-resistant component manufacturing and repair [7-8]. In the present work, two techniques: spark deposition and laser powder deposition, were used to deposit epitaxial layers onto single crystal substrates. Both techniques are compared and their advantages and disadvantages are highlighted.

Experimental procedure

High-energy micro-arc alloying was performed using a MD-WKD-1500 1.5kw constructed in the laser processing research center (LPRC), Wuhan University of Science & Technology. The alloying was carried out by a hand-held gun in room temperature with argon protection. HEMAA was performed at 100V, 850W and 100Hz. The revolving electrode was successively in traveling contact with the substrate surface to form thick Ni20Cr12Al and Rene N4 layers. The Rene N4 electrodes were produced by Nippon Welding, Japan, by plasma transferred arc (PTA) technique. The base plate dimensions were 20mm×20mm×3mm and the surface area was effectively covered within 3 minutes. The substrates were made from CMSX-4 single crystal Ni-based superalloy. The composition of the material can be seen in Table 1.

A Truedisk 4006 laser (max power of 4 KW and wavelength of 1030 nm) from Trumpf equipped with a TGV's double hopper powder feeder, a three beam coaxial powder nozzle and Kuka's KR-60HA robot arm was used for the laser deposition experiments. The deposits were made at laser power of 500 W, powder feed rate 1 g/min and laser 4mm/s scanning speed. The powder material was a modified 5th generation alloy of high Re and Ru content and the substrate was made of TMS 138A. The composition of the powder and substrate can be seen in Table 2.

The clad microstructure and crystallography were analysed by laser confocal microscope Keyence VK9700, Hitachi FEG-SEM SU6600 equipped with EDAX SDD XR-EDS and TSL Digiview electron backscatter diffraction detector. The EBSD measurements were performed at different step sizes ranging from 50 nm to 5 μm and probe current 7 nA. The crystallography of both the layers and the substrate was also analysed by X-ray diffraction using a Bruker D8 discover with GADDS. The

X-ray tube equipped with Cu or Cr radiation was operated at 40 kV/40 mA and 35 kV/40 mA, respectively. A graphite monochromator was used at the incident beam. The distance of the 2D detector and the X-ray tube source was 15 cm, this corresponds to a ±15° range from the centre of the detector.

Table 1 Substrate and powder used for spark deposition

wt%	Ni	Cr	Co	Mo	W	Al	Ti	Ta	Hf	Re	Nb	Fe	C
CMSX-4	61.8	6.5	9.0	0.6	6.0	5.6	1.0	6.5	0.1	3	n.a.	n.a.	n.a.
Rene N4	61.5	9.8	7.6	1.6	6.1	4.4	3.4	4.9	0.17	n.a.	0.5	0.08	0.06

Table 2 Substrate and powder used for laser deposition

wt%	Ni	Cr	Co	Mo	W	Al	Ti	Ta	Hf	Re	Ru	C	B
TMS-138A	61.8	3.2	5.8	2.8	5.6	5.7	n.a	5.6	0.1	[illegible]	3.6	n.a.	n.a.
modTMS	59.6	3.9	5.1	3.0	5.9	6.2	0.7	5.2	0.18	[illegible]	[illegible]	[illegible]	0.05

Experimental results and discussions

The spark deposited layers made by using NiCrAl and Rene N4 alloys can be seen in Figure 1. The layers were from 100 to 300 µm thick. It is posssible to see very good metallurgical bonding of layers with no porosity, however a few cracks can be observed. The layers made by using NiCrAl material had very high texture as shown in the X-ray diffraction pattern in Figure 2, however many stray grains could be observed as in the orientation imagine mapping in Figure 3. On the other hand, the layers made by using the Rene N4 material were of a mono-crystaline nature as shown in Figure 4. The misorientation profiles along the substrate material and from the bottom to the top of the deposited layer are shown in Figure 4b and 4c respectively. The highest "point-to-origin" misorientiom was 1.8° and 3° for the substrate and deposited layer. The formation of stray grains in Figure 1 was probably caused by the quality of the substrate. In the case of the deposits made with NiCrAl, the misorientation profile in the substrate showed a 18° maximum "point-to-origin" misorientation.

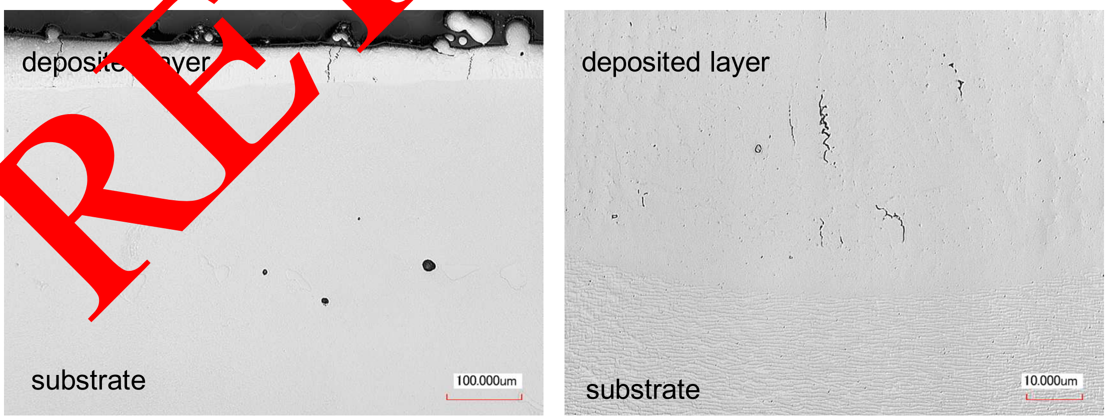

(a) (b)

Figure 1 Cross section of spark deposited layers: (a) NiCrAl layer (b) Rene N4 layer.

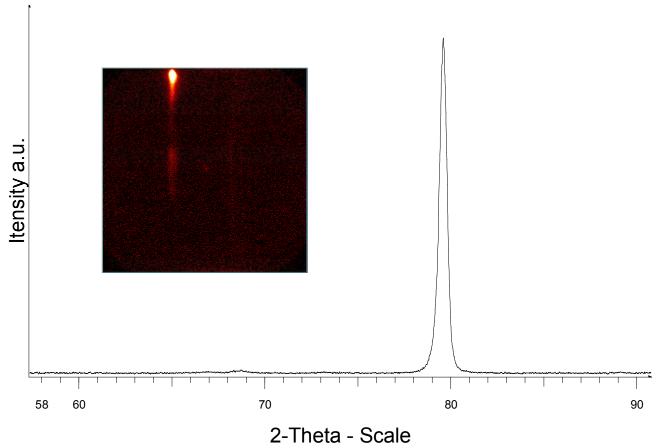

Figure 2 Diffraction pattern of NiCrAl layer showing high (100) texture of the deposited layer. Collimator size is 20 μm.

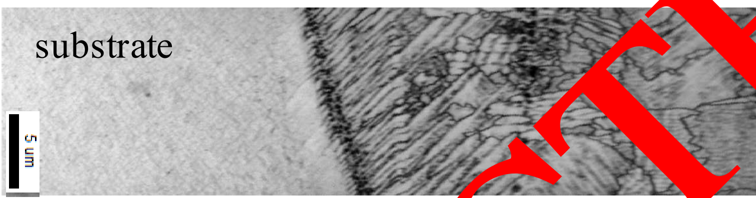

Figure 3 OIM (image quality map) showing strain grain formation close to the substrate/spark deposited layer interface. NiCrAl deposited onto CMSX-4 by spark deposition.

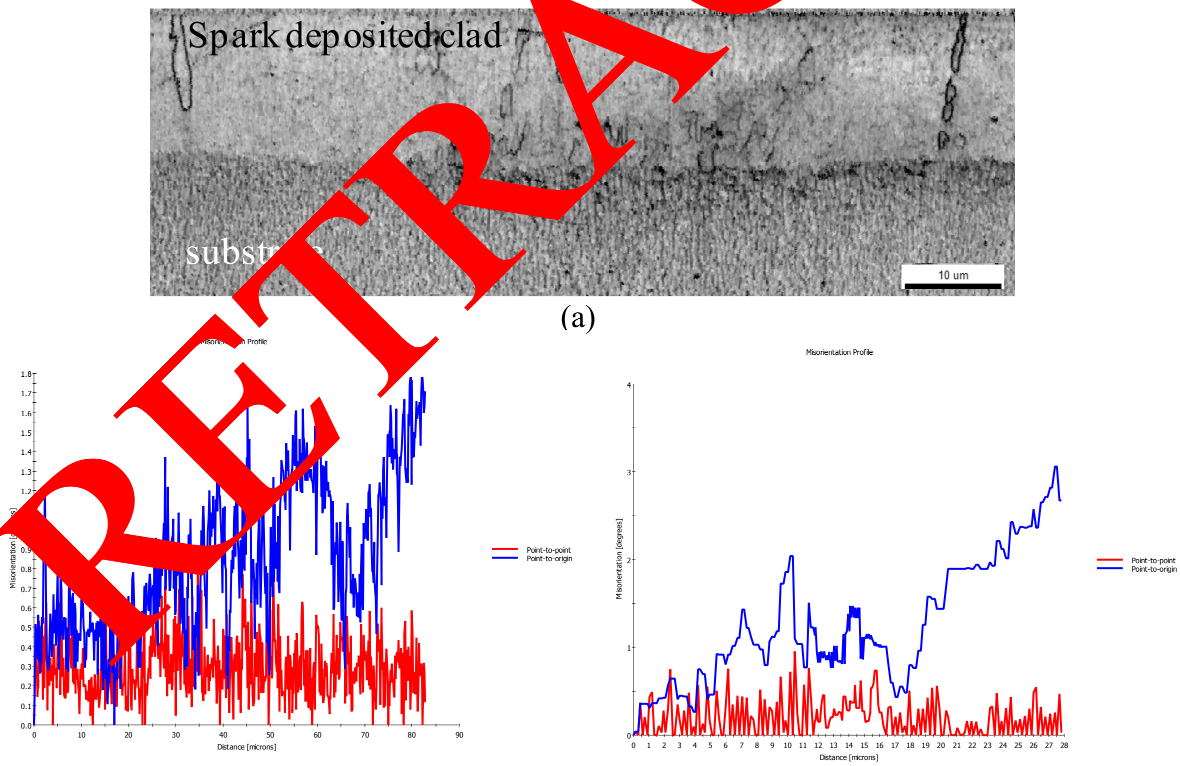

(b) (c)

Figure 4 OIM measurements of Rene N4 deposits onto CMSX-4 substrate: (a) image quality (b) misorientation profile along the substrate (max 1.8°) (c) misorientation profile from the substrate to the spark deposited layer top (max 3°).

Figure 5 shows the one-layer clad made by laser powder deposition onto TMS 138A substrates. The processing parameters were: laser power 500 W, laser beam diameter 2 mm, powder feed rate 1 g/min and laser scanning speed 4 mm/s. The clad shows almost no pores or cracks but high dilution and consequently high heat affected zone (HAZ) were observed. High dilution can be avoided by using lower power, higher powder feed rate and/or faster scanning speed [5, 9-12]. The substrate-laser deposited layer interface can be seen in Figure 5b. The planar front solidfication and dendritic growth can be clearly observed. The formation of a plane solidification front region at the bottom of track occurred due to the large temperature gradient (G) and low solidification rate (R) that existed in the bottom of the melt pool, during the first stage of solidification [5]. The solid-liquid interface rapidly evolves to a dendritic interface as solidification proceeds, due to the rapid decrease of the G/R ratio, which leads the formation of a constitutional undercooling region ahead of the S/L interface [5].

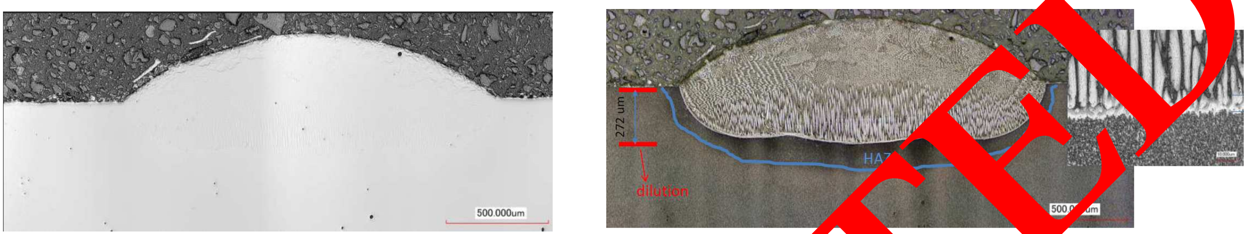

(a) (b)

Figure 5 LCM cross section micrographs of one-layer modTMS layer deposited samples onto TMS 138A substrate: (a) polished surface (b) etched sample and micrograph detail of the interface.

(a) (b)

Figure 6 Cross section of multiple build-up of modTMS alloy after laser powder deposition onto TMS 138A substrate: (a) polished and (b) etched sample. See detail of the layer-to-layer interface

During multiple-layer deposition, the previous layer is partially remelted when the following one is deposited, and this way epitaxial growth and crystallographic orientation are maintained across the successive layers. For adequate range of processing parameters, the columnar dendritic structure is preserved from layer to layer as well. As a result, multilayers present a dendritic structure where dendrites grow throughout the layers, as observed in Figure 6, an LCM micrograph of a multilayer sample deposited in [100] direction and a (001) surface substrate. The clads had very good metallurgical bonding and no pores or minimum cracks were observed.

Conclusions

Spark deposition and direct metal laser deposition were used to produce thick layers onto CMSX-4 and TMS 138A single crystal substrates. Both techniques showed a potential to produce single crystal clads by epitaxial forming onto single crystal substrates. The processing parameters for spark deposition still need to be optmised in order to avoid cracking and in the case of laser forming - to avoid high dilution. Laser deposition can produce thicker layers, however the initial cost of the machine significantly higher than the cost of a spark deposition device. Laser deposition is expected to be applicable when large areas require repair, while spark deposition can be used to formation of NiCrAl coatings or minor repair work.

Acknowledgements

We would like to thank Mr. Kaneyasu and Mr. Yamaguchi from Aichi Sangyo for the laser deposition trials. The authors would also like to thank Dr. Suzuki from TSL Japan for the EBSD data, Dr. Hiroshi from Bruker Japan for the X-ray data and Mr. Kobayashi from Keyence for the laser confocal microscopy measurements.

References

[1] R. C. Reed, The Superalloys, Fundamentals and Applications, Cambridge University Press, 2006, p. 372.

[2] H. M. Flower, High Performance Materials in Aerospace, Chapman & Hall, 1995.

[3] F. L. Versnyder, M. E. Shank, Materials Science and Engineering 6 (1970) 213-247.

[4] S. S. Babu, S. A. David, J. W. Park, J. M. Vitek, Joining of nickel-base superalloy single crystals, in: The Microsctructure and Performance of Joints in High-Temperature Alloys, The Institutute of Materials, Minerals, and Mining, IOM3, London, Uk, 2002.

[5] R.Vilar,E.C.Santos,P.N.Ferreira, N.Franco, R.C.Da silva, Acta mater, 57(2009)

[6] C. Chen, M. Zhang, S. Zhang, Q. Chang, X. Chen, Advanced Science Letters, Volume 4, Number 3, March 2011 , pp. 996-1001(6).

[7] R. Vilar, Journal of Laser Applications 11 (1999) 64-79.

[8] R. Vilar, Laser Alloying and Laser Cladding, in: R. P. Agarwala (Ed.) Lasers in Materials, Trans Tech Publications Ltd., 1999, pp. 229-252.

[9] C. Bezençon, J.-D. Wagnière, S. Mokadem, M. Konter, W. Kurz, Laser Processing of Single Crystal Superalloys, in: Laser Assisted Net Shape Engineering 3, Proceedings of the LANE 2001, Erlangen, Germany, 2001, pp. 211-222.

[10] M. Gäumann, C. Bezençon, P. Canalis, W. Kurz, Acta Materialia 49 (2001) 1051-1062.

[11] M. Gäumann, S. Henry, F. Cléton, J.-D. Wagnière, W. Kurz, Mater. Sci. Eng. A 271 (1999) 232-241.

[12] S. Mokadem, C. Bezençon, J.-M. Drezet, A. Jacot, J.-D. Wagnière, W. Kurz, Microstructure control during single crystal welding and deposition of Ni-base superalloys, in: M. M. S. The Minerals (Ed.) TMS annual meeting 2004, Charlotte, USA, 2004.